

This author's accepted manuscript may be used for non-commercial purposes in accordance with [Wiley Terms and Conditions for Self-Archiving](#).

The full details of the published version of the article are as follows:

TITLE: Tempo and mode of performance evolution across multiple independent origins of adhesive toe pads in lizards

AUTHORS: Travis J. Hagey, Josef C. Uyeda, Kristen E. Crandell, Jorn A. Cheney, Kellar Autumn, Luke J. Harmon

JOURNAL: Evolution

PUBLISHER: Wiley

PUBLICATION DATE: October 2017

DOI: [10.1111/evo.13318](https://doi.org/10.1111/evo.13318)

27 **Abstract**

28 Understanding macroevolutionary dynamics of trait evolution is an important endeavor in
29 evolutionary biology. Ecological opportunity can liberate a trait as it diversifies through trait
30 space, while genetic and selective constraints can limit diversification. While many studies have
31 examined the dynamics of morphological traits, diverse morphological traits may yield the same
32 or similar performance and as performance is often more proximately the target of selection,
33 examining only morphology may give an incomplete understanding of evolutionary dynamics.
34 Here we ask whether convergent evolution of pad-bearing lizards have followed similar
35 evolutionary dynamics, or whether independent origins are accompanied by unique constraints
36 and selective pressures over macroevolutionary time. We hypothesized that geckos and anoles
37 each have unique evolutionary tempos and modes. Using performance data from 59 species, we
38 modified Brownian Motion (BM) and Ornstein-Uhlenbeck (OU) models to account for repeated
39 origins estimated using Bayesian ancestral state reconstructions. We discovered that adhesive
40 performance in geckos evolved in a fashion consistent with Brownian Motion with a trend,
41 whereas anoles evolved in bounded performance space consistent with more constrained
42 evolution (an Ornstein-Uhlenbeck model). Our results suggest that convergent phenotypes can
43 have quite distinctive evolutionary patterns, likely as a result of idiosyncratic constraints or
44 ecological opportunities.

45

46 **Introduction**

47 When investigating how the diversity (or lack thereof) of a trait arose, one of the first steps is to
48 observe the variation present in the trait and investigate how the trait evolved through time,
49 asking whether the trait has thoroughly explored a small part of trait space, or if the trait appears
50 to have freely explored trait space. Thorough coverage of a limited region of trait space can
51 suggest constrained evolution, possibly due to limited developmental or genetic variation,
52 biomechanical constraints, or limited ecological opportunity to adapt and change. Alternatively,
53 a trait may appear to have explored trait space in a less constrained fashion. This may be due to
54 fewer developmental, genetic, or biomechanical constraints, the trait accessing more open
55 niches, or the trait being under weak selection, drifting through trait space with little
56 consequence.

57 Knowledge of how a clade has evolved through trait space can be integrated into a fuller
58 understanding of that clade's evolutionary history. If a clade has exhibited constrained
59 evolutionary patterns, future studies can investigate how the focal trait may be limited by
60 developmental, genetic, or mechanical constraints, or how biotic interactions have influenced the
61 diversification of the trait. For example, habitat use/morphology correlations have been reported
62 to differ between Caribbean and South American anoles (Irschick et al. 1997; Macrini et al.
63 2003). These differences may suggest Caribbean and mainland anoles have filled trait space
64 differently, possibly due to differences in development, genetics, biomechanical considerations,
65 or differences in abiotic or biotic conditions in the Caribbean and mainland South America.

66 In addition, morphological traits can be constructed in alternative ways to accomplish the
67 same adaptive function, and these alternative constructions may or may not require similar
68 amounts of morphological change to enable the organism to adapt to changing adaptive
69 requirements. For these reasons, studying performance directly as a trait, as is the case in our
70 study, rather than morphology may give a clearer picture of ecological function and evolutionary
71 dynamics (Arnold 1983; Wainwright and Reilly 1994). Evidence of a clade having evolved
72 constrained in performance space could be explained by a variety of situations. Focal clades may
73 not have had the genetic, developmental, or mechanical capabilities to diversify and explore
74 performance space, or there may have been limited niche space available to diversify into,
75 similar to as if a focal trait was a morphological trait. In addition, when considering performance
76 niche space, limited successful performance options do not impose limited underlying
77 morphological diversity. Few adaptive options can lead to convergent or parallel morphological
78 evolution, including many-to-one mapping, when different morphologies perform similarly.
79 Alternately, evidence of unconstrained-performance evolution could be explained by behavioral
80 plasticity, phenotypic plasticity, adaptive change tracking adaptive peaks, as well as weak
81 selection allowing performance to drift through performance space.

82 Modeling the evolutionary history of a trait also requires some knowledge or assumptions
83 about the origin or origins of the trait in question. While many studies have focused on the
84 relationship between convergent morphology and performance, few studies have compared the
85 tempo and mode of performance evolution in a comparative framework (but see Harmon et al.
86 2003). By focusing on convergent traits, we can better understand how limiting factors such as
87 constraints or limited ecological opportunities have shaped the evolution of our focal clades.

88 Evaluating the fit of Ornstein-Uhlenbeck (OU) and Brownian motion (BM) models of
89 trait evolution to a focal clade can identify how constrained (OU) or unconstrained (BM) the
90 evolution of the trait has been (Lande 1976; Hansen 1997). Brownian motion models the
91 diffusion of a trait through trait space with two parameters, the root value and a stochastic rate
92 parameter (σ^2). Alternatively, OU models extend BM models to represent constrained evolution
93 towards a target value (θ). OU has the additional parameter α , which describes the rate of pull
94 towards the target trait value θ . As α gets smaller and approaches zero, an OU model converges
95 towards a BM model. BM models can also be extended to model a directional trend when a third
96 parameter, μ , is non-zero, modeling the tendency of the trait value to consistently drift in a
97 particular direction (positively or negatively) away from the root value.

98 In this study, we examine the evolutionary dynamics of performance in two groups of
99 squamates: geckos and anoles. Adhesive toe-pads have evolved at least three times in Squamata:
100 most famously in geckos, but also twice outside of Gekkota, in anoles and skinks. We define
101 adhesive toe pads as having morphological traits such as setae or modified scales that generate
102 both friction and adhesion (frictional adhesion; Autumn et al. 2006a). The results from previous
103 studies have suggested one (Harrington and Reeder 2017) or multiple origins of toe pads within
104 the 1700 described species of geckos (Underwood 1954; Haacke 1976; Russell 1976; Russell
105 1979; Irschick et al. 1996; Russell 2002; Gamble et al. 2012; Russell et al. 2015; Higham et al.
106 2016; Gamble et al. 2017). The adhesive system of lizards is an excellent system for
107 investigating patterns of adaptation, constraint, and convergence. Gecko and anole toe pads are
108 morphologically complex, being comprised of modified ventral scales with a free edge
109 (lamellae) covered in small hair-like structures called setae. There is considerable morphological
110 diversity among species at the macroscale *i.e.*, toe pad shape, skeletal features, and digital
111 musculature (Russell 1979; Gamble et al. 2012) and at the microscale *i.e.*, setal morphology
112 (Ruibal and Ernst 1965; Williams and Peterson 1982; Peattie 2007; Johnson and Russell 2009;
113 Hagey et al. 2014). These structures are responsible for generating adhesion and friction on a
114 variety of surface textures, self-cleaning, and not self-adhering (Hansen and Autumn 2005;
115 Vanhooydonck et al. 2005; Autumn et al. 2006a; Huber et al. 2007; Persson 2007; Russell and
116 Johnson 2007; Pugno and Lepore 2008b; Hu et al. 2012; Autumn et al. 2014; Russell and
117 Johnson 2014) suggesting that while toe pads appear very diverse, there likely exists extensive
118 constraints and limitations on their morphology and performance. It is likely that the evolution

119 and adaptation of adhesive performance in padded lizards has balanced selective pressures and
120 opportunities with mechanical and developmental constraints, likely limiting the options open to
121 evolution and adaptation.

122 We considered how gecko and anole toe pad adhesive performance evolved by fitting a
123 variety of stochastic models of trait evolution. We fit models with shared or independent
124 parameter values and/or models across geckos and anoles, incorporating ancestral state
125 reconstruction results into our models, to test the hypothesis that independent origins differ in
126 rate (tempo) or pattern (mode). If a single-rate model is a good fit to our entire adhesive
127 performance dataset, this would suggest that the performance of padded lizards and their
128 convergent morphologies evolved under similar processes, shared mechanical, developmental
129 constraints, and/or similar selection dynamics. In contrast, if clade-specific models or parameters
130 fit our data well, this would reveal a pattern of clade-specific evolutionary dynamics, likely
131 associated with clade-specific constraints or ecological opportunities (Hansen 1997; Butler and
132 King 2004; Yoder et al. 2010; Eastman et al. 2013). Considering patterns of performance
133 evolution in conjunction with ancestral information improves our understanding of how
134 historical processes of adaptation have shaped extant diversity, morphology, and performance.

135

136 **Methods.**

137 *Estimation of the number of origins of toe pads across Squamata*

138 To identify independent origins of adhesive toe pads in lizards, we used a large, species-level
139 phylogeny of Squamata (Pyron and Burbrink 2013). While this phylogeny has topological
140 differences as compared to other smaller, group-specific phylogenies (Sadler et al. 2005; Brown
141 et al. 2012; Gamble et al. 2012; Oliver et al. 2012), we do not feel these differences impacted our
142 results. Also see Title and Rabosky (2016) for comments on the use of large macrophylogenies
143 in diversification studies. We chose a time-scaled, ultrametric phylogeny because our models of
144 trait evolution model trait change in relation to time rather than sequence divergence. We
145 assigned presence or absence of toe pads to each species in the phylogeny (4162 species). Four
146 species of skinks are known to have adhesive pads, *Prasinohaema virens*, *P. flavipes*, *P.*
147 *prehensicauda*, *Lipinia leptosoma* (Williams and Peterson 1982; Irschick et al. 1996; Pianka and
148 Sweet 2005). Of the three pad-bearing *Prasinohaema* species, only *P. virens* is in the Pyron and
149 Burbrink (2013) phylogeny. In addition, only one species of *Lipinia* is in the phylogeny (*L.*

150 *pulchella*). We substituted *L. leptosoma* for *L. pulchella* without a loss of phylogenetic
151 information (Austin 1998) for a total of two pad-bearing skink species in our toe pad
152 presence/absence dataset. We assigned the presence of toe pads to all *Anolis* species in the
153 phylogeny (207 species) except *A. onca* (Peterson and Williams 1981; Nicholson et al. 2006). To
154 assign presence/absence to geckos, we modified generic-level assignments from Gamble et al.
155 (2012) adding information from Wilson and Swan (2010) and personal observations (TH), to
156 assign toe pad presence (472 species) or absence (188 species) to all 660 species of geckos in the
157 phylogeny (see Fig. 3 and Supplemental Material). The remaining lizard and snake species in the
158 tree were considered padless.

159 Using the complete phylogeny of Pyron and Burbrink (2013), we estimated the number
160 of origins of adhesive toe pads across squamates by combining Bayesian estimates of transition
161 rate matrices with stochastic character mapping. We estimated transition matrices for a binary-
162 state, Mk model with asymmetric transition rates allowing the rates of pad gain and loss to vary
163 (*i.e.*, q_{10} and q_{01} were not constrained to be equal) using the R package Diversitree (FitzJohn
164 2012). We then ran a Bayesian MCMC for 10,000 generations sampling every 100 generations,
165 with an initial burn-in of 3,000 generations, resulting in a posterior sample of 701 Q matrices. To
166 visualize our reconstructions, monomorphic clades were collapsed, resulting in a phylogeny with
167 118 tips. Using the posterior sample of Q-matrices, we generated 701 simmap phylogenies using
168 the R function *make.simmap* in the phytools package (Revell 2012). Of particular interest was
169 the number of independent origins of toe pads within geckos (Gamble et al. 2012). We therefore
170 counted the number of estimated origins in Gekkota across the simmap-generated
171 reconstructions to obtain a posterior sample of origins.

172

173 *Collection of performance data*

174 Previous studies of pad-bearing lizards have quantified adhesive performance in multiple ways
175 (Irschick et al. 1996; Autumn et al. 2006a; Autumn et al. 2006b; Pugno and Lepore 2008a;
176 Autumn et al. 2014; Hagey et al. 2014; Hagey et al. 2016). We chose to use the angle of toe
177 detachment, which was first used to quantify adhesive performance in frogs (Emerson 1991;
178 Moen et al. 2013) and subsequently in geckos (Autumn et al. 2006a; Hagey et al. 2014; Hagey et
179 al. 2016). The angle of toe detachment is directly related to the adhesive mechanics of setae
180 (Autumn et al. 2006a; Tian et al. 2006) and can be measured easily in the laboratory or field with

181 relatively simple equipment (see Supplemental Material). This approach quantifies the maximum
182 proportion of adhesion (negative normal force), relative to friction, generated by a species' toe
183 pad (see Fig. 1 and Methods). We quantified adhesive performance across three families of
184 geckos (Gekkonidae, Phyllodactylidae, and Diplodactylidae) and the genus *Anolis* (see
185 Supplemental Material). Our toe detachment observations were collected following previous
186 studies, using captive and wild caught specimens from the field (Costa Rica, Panama, Thailand,
187 and Australia) and the lab (Autumn et al. 2006a; Hagey et al. 2014; Hagey et al. 2016). We used
188 a variety of equipment setups that included powered rotational stages, stepper motors (including
189 Lego Mindstorm motors), and manual rotational stages. To measure angle of toe detachment,
190 live non-sedated lizards were suspended via the toe pad of a single rear toe from a vertical glass
191 microscope slide (Video links in Supplemental Material; Autumn et al. 2006a; Hagey et al. 2014;
192 Hagey et al. 2016). Variation in performance across toes has not been previously investigated
193 and so we strived to always test similar toes. Our trials alternated between the longest left and
194 right rear toes, or the center rear toes if all rear toes were similar in length. Using a single toe
195 eliminated confounding forces that would be generated by multiple toes acting in opposing
196 directions. During each toe detachment trial, the glass substrate was initially vertical with the
197 animal's toe pad generating friction relative to the substrate (and likely little adhesion *i.e.*, force
198 perpendicular and towards the glass). The glass substrate was then slowly inverted. When this
199 occurred, the setal shaft angle increased, generating adhesion and friction relative to the glass. At
200 the angle of toe detachment, the maximum ratio of adhesion to friction that the toe pad was
201 capable of generating was exceeded, and the animal fell onto a cushioned pad (see Fig. 1 and
202 video links in Supplemental Material). Toe-pad area has previously been shown to correlate with
203 the amount of friction generated by anole toe pads (Irschick et al. 1996), presumably due to the
204 fact that larger pads have more setae interacting with the substrate. This relationship has not been
205 investigated regarding toe detachment angle. While we would not predict toe-pad area to
206 correlate with toe detachment angle, due to the fact that detachment angle is weight independent
207 and likely related to setal morphology (Autumn et al. 2006a) and not the absolute number of
208 setae contacting the surface, this relationship still requires evaluation.

209 Our performance observations included measurements of over 250 individual lizards
210 from 59 species (13 species of anoles and 46 species of geckos; Fig. 3; see Supplemental
211 Material). Our dataset had a minimum of two observations per individual and maximum of 49,

212 with a mean of 9.1 observations per individual. We collected five or more observations from
213 91% of the individuals sampled. Observations from each individual lizard were fit to a Weibull
214 distribution, which is often used in “time-to-failure” analyses (McCool 2012). The Weibull scale
215 parameter, with standard error, was then estimated, representing each individual’s detachment
216 angle (Hagey et al. 2016). To produce a mean value for each species, we calculated a weighted
217 average using each individual’s estimated Weibull scale value, weighting by the inverse of its
218 estimated standard error. In six of our 59 focal species, we did not record individual identity for
219 each performance trial; therefore we estimated performance of these species as if all observations
220 were from a single individual (see Table S.1).

221

222 *Modeling trait evolution*

223 We performed all trait evolution analyses using untransformed performance data.
224 Natural-log transforming our data would artificially emphasize differences between small
225 detachment angles and reduce differences between large detachment angles. Our initial analyses
226 fit single and multi-regime BM and OU models of trait evolution via a maximum likelihood
227 approach with the use of *a priori* assigned clades using the R package OUwie (Beaulieu et al.
228 2012). We also conducted analyses not requiring *a priori* clade assignments using the R
229 packages AUTEUR (Eastman et al. 2011), fitting multi-regime BM models, and SURFACE
230 (Ingram and Mahler 2013), fitting multi- θ OU models (See Supplemental Material). In our
231 OUwie analyses we considered seven models in total, including species mean errors. Our two
232 simplest models were a Brownian motion model (BM1) and an Ornstein-Uhlenbeck model
233 (OU1) that each fit a single set of parameters. Our other five models fit unique parameter values
234 in various combinations to the gecko and anole clades. The decision to assign unique parameter
235 values to anoles and geckos followed the results obtained from our ancestral state reconstruction,
236 with anoles and geckos representing independent origins of toe pads, although we note that other
237 studies have suggested multiple independent origins within geckos (see Introduction and
238 Discussion). We fit the following models: a BM model with variable evolutionary rates (σ^2) and
239 single root value (BM σ^2), an OU model with single α and σ^2 parameter value and different
240 optima (θ) values (OU θ), an OU model with a single α but multiple rate (σ^2) and optima (θ)
241 parameter values (OU $\sigma^2\theta$), an OU model with a single σ^2 but variable α and θ values (OU $\alpha\theta$),
242 and a OU model (OU $\sigma^2\alpha\theta$) in which all three parameters, σ^2 , α , and θ , varied (Table 1; Beaulieu

243 et al. 2012). We then compared the fit of our seven models using AICc weights based on relative
244 model likelihoods (Table 1; Burnham and Anderson 2002).

245 The models we have described so far can sometimes rely on unrealistic assumptions.
246 These models estimate a trait value at the root, which is the phylogenetic weighted mean of tip
247 states for our BM1 and OU1 models. In our case, toe pads have had multiple origins, with the
248 backbone of the squamate phylogeny likely lacking toe pads. Our model assumptions regarding
249 performance at the root of the tree, the most recent shared common ancestor of geckos and
250 anoles, is inferred to have a performance that is near the average of geckos and anoles. This is
251 almost surely in error. Incorrect root-node trait values can affect parameter estimate values and
252 fit comparisons; for example, by allowing less change and/or a weaker α parameter value,
253 mimicking Brownian Motion. To incorporate ancestral state information, we fit a set of BM and
254 OU models that assumed independent origins for geckos and anoles using modified likelihood
255 functions from the R packages *bayou* and *geiger* (Harmon et al. 2008; Pennell et al. 2014; Uyeda
256 and Harmon 2014). We considered the lack of toe pads to have a performance value of 0° . Both
257 the gecko and anole clades were assigned a root state of 0° and shifted to an OU or BM process
258 model along their respective stem branch, with the timing of the initiation of the OU or BM
259 model being allowed to vary along the branch, before diversification. When considering the
260 likely evolution of setae from spinules, simple early structures likely initially generated friction
261 but little adhesion, which would present itself as a low detachment angle. Higher detachment
262 angles were likely achieved after the evolution of more complex setae (see Discussion). As a
263 result, our assignment of detachment angles of 0° to padless species and the assumption that
264 recently evolved toe pads have performance near zero is supported from a biomechanical and
265 evolutionary point of view.

266 Stem branch dates were taken from the Pyron and Burbrink (2013) phylogeny. For
267 geckos, the timing of the shift to an OU or BM process was constrained to occur between 168.8
268 mya (the timing of the divergence of geckos from other lizards) and 82.3 mya (the ancestral node
269 of Gekkota). For anoles, the timing of the shift was constrained between 76.3 mya (the
270 divergence of anoles from Corytophanidae) and 44.1 mya (the ancestral node of *Anolis*). We
271 again considered single and multi-regime models of BM and OU, constraining our OU models to
272 a maximum θ value of 90° (no species has been observed sticking to a surface with one toe
273 beyond an angle of 45°). A total of 9 models incorporating ancestral information were

274 considered (models denoted by an asterisk, Table 1). We did not exhaustively fit all possible
275 combinations of models, but instead let the results of earlier analyses guide our choices: BM with
276 a shared σ^2 for both geckos and anoles (*BM1), Single-optimum OU with shared α and σ^2
277 parameters (*OU1), Brownian motion with a trend and shared mean, σ^2 , and μ parameter, where
278 μ describes the rate of the trend (*BMT), Brownian motion with a trend and shared σ^2 , but
279 different trend (μ) parameters for each clade (*BMT μ), an OU model with separate θ for each
280 clade (*OU θ), OU with separate α and θ for each clade (*OU $\alpha\theta$), OU with separate σ^2 and θ for
281 each clade (*OU $\sigma^2\theta$), OU with separate α , σ^2 , and θ for each clade (*OU $\sigma^2\alpha\theta$), and lastly a BM
282 model with a trend fit to geckos and an OU model fit to anoles (*BMT_G-OU_A). We computed
283 AIC scores and AIC weights for each model using maximum likelihood optimization to evaluate
284 which model was best supported by our data (Table 1). To supplement these analyses assuming
285 one origin of toe pads within geckos, we also conducted a set of limited analyses assuming two
286 origins of toe pads within Gekkota (see Supplemental Material).

287 In addition to this likelihood analysis, we fit the full *OU $\sigma^2\alpha\theta$ model using a Bayesian
288 implementation in *bayou* (denoted *OU $\sigma^2\alpha\theta$ _{Bayesian} in Table 1). By considering our most complex
289 model, we can compare posterior probabilities for inferring differences in parameters between
290 clades. We set the following priors on the parameters: $\alpha \sim$ half-Cauchy(scale = 0.1), $\sigma^2 \sim$ half-
291 Cauchy(scale = 0.1), $\theta \sim$ Uniform(min = 0, max = 90). Shift locations were given uniform priors
292 over the length of the stem branches for geckos and anoles. We ran four chains for 1,000,000
293 generations and discarded the first 30% of the samples as burn-in. We then combined all the
294 chains and estimated the median and 95% highest posterior density (HPD) interval for each
295 parameter value.

296 For use in our comparative modeling, we modified the Pyron and Burbrink (2013)
297 phylogeny by removing unsampled taxa. In a few cases we replaced closely related unsampled
298 taxa with taxa for which we had performance measurements. We replaced *Afroedura karroica*
299 and one of the closely related *Geckolepis* species with *A. hawequensis* and *A. loveridgei*,
300 possibly overestimating the divergence between our two sampled *Afroedura* species. We also
301 had performance observations from the recently described *Oedura bella*, substituting it for the
302 closely related *O. gemmata* (Oliver et al. 2012; Oliver and Doughty 2016).

303

304 **Results**

305 Regarding our reconstruction of the number of independent origins of toe pads, our posterior
306 sample of transition matrices had negligible autocorrelation for all parameters and high effective
307 sample sizes, indicating convergence and adequate mixing. Transition rates were estimated to be
308 highly asymmetric, with losses of toe pads occurring at rates an average of 16.8 times faster than
309 gains (95% HPD 3.2 – 41.1). Our reconstruction favored three origins in squamates (geckos,
310 anoles, and skinks, Fig. 2) but we were unable to rule out multiple origins within geckos. Within
311 geckos, our reconstruction favored a single origin (53% of posterior reconstructions), followed
312 by two origins (30%), with only 4% of reconstructions having three or more origins within
313 geckos. 13% of our reconstructions contained no origins within geckos, modeling the root of
314 squamates as having pads. It is worth noting that we observed some reconstructions in our
315 posterior sample with transient assignments, in which toe pads transitioned from absent to
316 present, back to absent along a single branch, generating no overall change but possibly inflating
317 the number of origins we observed. In addition, we observed an origin of toe pads in the branch
318 leading to *Hemidactylus* in 33% of our posterior reconstructions, complementing previous
319 studies of toe pad origins in geckos (Fig. 2; Gamble et al. 2012).

320 We conducted a Shapiro-Wilk test of normality and found our performance data to not be
321 significantly different from than expected for a normal distribution ($W = 0.98$, $p = 0.32$). We
322 found toe detachment angle to vary widely across padded lizards (Fig. 3, Table S.1), ranging
323 from 15° to over 40° . When we consider detachment angle among clades, we note detachment
324 angle in anoles ranged from 15.7° to 23.3° ; lower than in most gecko species. Gekkonid and
325 phyllodactylid geckos showed the greatest variation, with detachment angles ranging from 23.4°
326 to 40.5° (Fig. 3, Table S.1). Diplodactylid geckos exhibited intermediate performance between
327 anoles and the gekkonids and phyllodactyls, exhibiting detachment angles between 15.0° and
328 30.1° (Fig. 3, Table S.1).

329 Considering our trait evolution analyses, our OUwie results did not find clear support for
330 one particular model of trait evolution (Table 1). We found support for a single-rate BM model
331 (BM1, AICc weight of 0.35) with weaker support for an OU model with clade specific σ^2 , α , and
332 θ values, (OU $\sigma^2\alpha\theta$ model, AICc weight of 0.19). When we examine our OU $\sigma^2\alpha\theta$ model
333 parameter estimates, geckos were modeled under an OU model with a very small α value
334 (2.1×10^{-9}), large σ^2 (3.6), and distant θ (> 1000), which converges towards BM with a trend

335 (Table 1). It is worth noting again that these models assume unrealistic ancestral states, with a
336 phylogenetic mean performance value for the ancestor of geckos and anoles, which almost
337 certainly did not have toe pads.

338 For our custom models of trait evolution, which improved upon our OUwie analyses by
339 incorporating constrained root state and timing of parameter shifts, our best fitting model was
340 one in which geckos evolved under a BM model with a trend, and anoles evolved under an OU
341 model (*BMT_G-OU_A, AIC weight = 0.37; Fig. 4), followed closely by a global Brownian Motion
342 with a trend model (*BMT, AIC weight = 0.35; Table 1). The third best-fitting model assigned
343 unique μ values to geckos and anoles (*BMT μ , AIC weight = 0.18). When independent OU
344 models are fit to geckos and anoles, the estimated gecko phylogenetic half-life was 208.2 million
345 years with an estimated θ of 90° (the maximum allowable performance value), compared to the
346 short half-life estimated for anoles of 0.33 million years and a θ of 19.4°. Support for a BM
347 model with a trend in geckos is indicative of very little statistical signal for bounded evolution, a
348 surprising result given the bounded nature of performance space (detachment angle being
349 constrained between 0° and 90°). This result is supported when assuming one or two origins in
350 Gekkota (see Supplemental Material). By contrast, there is support for an OU model in anoles, in
351 which anoles are very near their estimated θ value and have a very rapid phylogenetic half-life.
352 However, possibly due to the limited sampling of *Anolis* species in our dataset (14 species), the
353 *BMT and *BM_G-OU_A models are roughly equivalent when accounting for the fact that the
354 *BMT model has only four parameters, while the *BM_G-OU_A model has seven.

355 Considering our *OU $\sigma^2\alpha\theta_{\text{Bayesian}}$ model, although we observed overlap among parameters
356 estimated for geckos and anoles, the results again suggest that the phylogenetic half-life for
357 anoles is shorter than that of the geckos, with anoles much closer to their θ value, whereas gecko
358 evolution is relatively unconstrained (Fig. 5; Table 1). All parameter estimates reached
359 stationarity and had effective sizes of over 200 and were similar to maximum likelihood
360 estimates (Table 1).

361

362 **Discussion**

363 In this study, we modeled the evolution of adhesive performance considering gecko and anole
364 lizards. In order to incorporate historical information such as the repeated evolution of adhesive
365 toe pads in lizards, we conducted an ancestral state reconstruction. Our reconstruction favored a

366 single origin of toe pads within geckos, which is significantly fewer than previous work (Gamble
367 et al. 2012), although we cannot rule out multiple origins (see Gamble et al. 2017). Our
368 performance observations suggested toe detachment angle to be highly variable across species of
369 padded lizards (14° to 40°, see Supplemental Material). Lastly our modeling results supported
370 our hypothesis that independent toe pad origins would exhibit different tempos and modes of
371 performance evolution. There was no evidence of substantial constraints on the evolution of
372 gecko adhesive performance. In fact, we found consistent support for an unconstrained model of
373 trait evolution in geckos, which indicates adhesive performance in geckos has evolved with
374 ample evolutionary opportunity and few constraints. Conversely, anole performance appears to be
375 limited to relatively low angles of toe detachment, suggesting strong constraints, consistent
376 selection, or limited ecological opportunity.

377

378 *Independent Origins of Toe Pads*

379 Many previous studies have contributed to our understanding of independent toe pad origins
380 within geckos (Underwood 1954; Haacke 1976; Russell 1976; Russell 1979; Irschick et al. 1996;
381 Russell 2002; Higham et al. 2015; Russell et al. 2015; Higham et al. 2016), with recent studies
382 suggesting between one (Harrington and Reeder 2017) and eleven origins (Gamble et al. 2012),
383 including origins in the Phyllodactylidae family and on the stem of *Hemidactylus*. This is still a
384 very active area of research (Gamble et al. 2017). Our reconstruction suggested a single origin at
385 the base of geckos, although we did find some evidence suggesting *Hemidactylus* may represent
386 an independent origin of toe pads within Gekkota (see Results, Fig. 2, and Supplemental
387 Material), complementing results from Gamble et al. (2012), despite topological differences
388 between the Gamble et al. (2012) and Pyron and Burbrink (2013) phylogenies regarding genera
389 closely related to *Hemidactylus* (see Title and Rabosky 2016 regarding the use of
390 macrophylogenies in comparative analyses). While neither our study nor the Gamble et al.
391 (2012) study allowed the rate of pad gain or loss to vary across clades, some clades may be
392 predisposed to evolving or losing adhesive toe pads, resulting in clade-specific rates of gain or
393 loss. There are multiple distantly related genera of geckos that exhibit adhesive structures on the
394 tips of their tails strikingly similar to those on their toes such as *Lygodactylus* in the Gekkonidae
395 family and New Caledonia and New Zealand genera in the Diplodactylidae family (Bauer 1998).
396 These independent origins of adhesive tail pads may suggest that geckos are predisposed to

397 evolve adhesive pads, possessing easily co-optable developmental pathways as compared to
398 other lizards.

399 In addition, if toe pad state is correlated with diversification rate, this may impact
400 ancestral reconstruction results (Maddison 2006). Gamble et al. (2012) found toe pads to be
401 associated with slightly higher rate of diversification, although this was not the case for Garcia-
402 Porta and Ord (2013). Considering state-correlated diversification rate alongside an ancestral
403 state reconstruction, Harrington and Reeder (2017) concluded a single origin of toe pads using a
404 ‘hidden states’ binary-state speciation and extinction model (Maddison et al. 2007; Beaulieu et
405 al. 2013; Beaulieu and O'Meara 2016), although Gamble et al. (2017) dispute these results due to
406 potentially high Type 1 error rates (Davis et al. 2013; Maddison and FitzJohn 2015; Rabosky and
407 Goldberg 2015). Future studies may want to consider incorporating character-state correlated
408 diversification information into ancestral state reconstructions using the recently published
409 nonparametric FiSSE (Fast, intuitive, State-dependent, Speciation-Extinction) approach
410 (Rabosky and Goldberg 2017; Zenil-Ferguson and Pennell 2017).

411 When considering other lines of evidence such as the variation in toe hyperextension
412 anatomy within geckos (Russell 1979), it is likely that the true number of origins within geckos
413 lies somewhere between one and many (Gamble et al. 2017). Future studies investigating the
414 origins of adhesive toe pads in lizards will benefit from considering multiple lines of evidence
415 (Gamble et al. 2017). The adhesive toe pads of lizards vary in toe pad shape, spinule/seta
416 morphology, skin-to-bone digital tendon system characteristics (Russell 2002), and the
417 presence/absence of internal blood sinuses and paraphalanges (Russell 1976; Russell and Bauer
418 1988; Gamble et al. 2012). The presence of epidermal spinules may predispose lizards to express
419 adhesive setae, with epidermal spinules having likely evolved into adhesive setae (Maderson
420 1970; Stewart and Daniel 1972; Russell 1976; Peterson 1983; Peattie 2008). Epidermal spinules
421 appear to be common across geckos and other lizards, including Chamaeleonidae, Iguanidae,
422 Leiocephalidae, and Polychrotidae (Maderson 1964; Ruibal 1968; Maderson 1970; Stewart and
423 Daniel 1975; Peterson 1984; Bauer and Russell 1988; Irish et al. 1988; Peattie 2008; Vucko
424 2008). Russell et al. (2015) provide a stunning example in *Gonatodes*, highlighting variation in
425 both setal and toe pad morphology suggesting that *Gonatodes* may represent an example of
426 elongated spinules and enlarged ventral scales performing as a friction-generating pad.

427

428 *Trait Evolution*

429 We used angle of toe detachment as a measure of adhesive performance because it has a well-
430 supported mechanistic basis (Autumn et al. 2006a; Tian et al. 2006), although other metrics exist
431 (Irschick et al. 1996; Irschick et al. 2006; Stark et al. 2012; Crandell et al. 2014). Using this
432 measure of performance, we saw striking differences between our focal clades. Species with the
433 lowest detachment angles (mostly anoles, near 15°) only produce a maximum of 0.27 units of
434 adhesion for one unit of friction, [using $\tan(\text{detachment angle}) = \text{adhesion/friction}$ (Autumn
435 et al. 2006a; Hagey et al. 2014)], whereas particular Gekkonidae geckos have detachment angles
436 over 40° and produce up to 0.84 units of adhesion for every unit of friction, over three times as
437 much as our lowest performing species.

438 Our trait evolution modeling analyses, which used modified models of trait evolution and
439 our ancestral state reconstruction results, suggested that our observed pattern of gecko
440 performance is well described by a BM with a trend model or a weak OU model with parameters
441 converging towards a BM with a trend (large σ^2 , distant θ , and small α values; Table 1; Fig. 4, 5).
442 Both models suggest adhesive performance in geckos has evolved directionally, yet relatively
443 unbounded. Conversely, our results suggest anoles, which are much younger than geckos,
444 evolved rapidly in a bounded sub-section of performance space, similar to a conventional OU
445 model (short phylogenetic half-life and a θ value near observed values; Table 1; Fig. 4, 5).
446 However, likely due to limited sample size, we have only weak evidence against a Brownian
447 Motion with a trend model.

448 These observed differences in performance and evolutionary tempo and mode mirror
449 anole and gecko macro- and micro-adhesive morphology, ecology, and the fossil record. For
450 example, geckos were found to be more variable in adhesive performance (Fig. 3) and also have
451 a much wider range of toe pad shapes, setal morphology (Peattie 2007; Gamble et al. 2012), and
452 ecology as compared to anoles. Geckos live in tropical, arid, and temperate environments on
453 rocks, vegetation, and terrestrial substrates, whereas anoles are generally found in arboreal
454 microhabitats in the Caribbean and South America. Mainland anoles have more detachment
455 angle diversity as compared to Caribbean anoles. These differences may be related to mainland
456 and Caribbean lizard community structure and ecological opportunity (Macrini et al. 2003; Losos
457 2009). As a result, geckos may be evolving within many different adaptive zones, while the
458 limited variation in the ecology of anoles may be driving them towards one or a few adaptive

459 zones without selecting for novel adhesive morphology. Further work exploring the relationship
460 between adhesive performance and habitat use of padded lizards is also crucial to place
461 performance reported here in an ecological context. Conversely, the evolvability of the gecko
462 and anole adhesive systems may be a driving factor, allowing geckos to diversify extensively,
463 and limiting anole toe pad shape, setal morphology, or performance and hence limiting them to
464 one or few adaptive zones. Our trait modeling results also complement studies of the fossil
465 record. Studies of trait evolution can sometimes underestimate ancestral trait diversity (Mitchell
466 2015), but recent fossil evidence from anoles preserved in amber suggests a model in which
467 anoles rapidly evolved their current phenotypes, with anole ecomorphs having changed little
468 since the Miocene (Sherratt et al. 2015). The gecko fossil record is unfortunately less informative
469 (Daza et al. 2014; Daza et al. 2016).

470 Our results provide an example of convergent traits evolving under different evolutionary
471 histories, highlighting the importance of considering macroevolutionary dynamics when
472 inferring historical contingency and ecological opportunity during adaptation. Our study also
473 describes the evolution of a performance trait instead of morphological traits. Despite our results
474 detailing strong evolutionary constraints on anole evolution that we did not find in geckos, there
475 remain many open questions as to how lizard adhesive toe pads have evolved, how they work,
476 and how they are used in the wild. Our results highlight the need to conduct more biomechanical,
477 ecological, and developmental studies of padded lizards with an explicit consideration of their
478 origins. Our results also illustrate the value in incorporating additional information into
479 comparative phylogenetic methods. Without the use of our modified *bayou* model, we would not
480 have identified differences between the evolution of performance in geckos and anoles and we
481 strongly encourage researchers to investigate their model assumptions.

482

483 **Acknowledgements**

484 We would like to thank the National Science Foundation in collaboration with Aaron Bauer and
485 Todd Jackman (Award #0844523), the National Geographic Society/Waitts Institute (Grant
486 #W216-12), the BEACON Center for the Study of Evolution in Action (Request #302, #429), the
487 NSF Collaborative Research grant: Arbor: Comparative Analysis Workflows for the Tree of Life
488 (Harmon et al. 2013), and Sigma XI (#G200803150489) for funding, Matt Pennell for helpful
489 discussions, Jon Eastman for help with analyses, Jon Boone for access to animals, Bobby

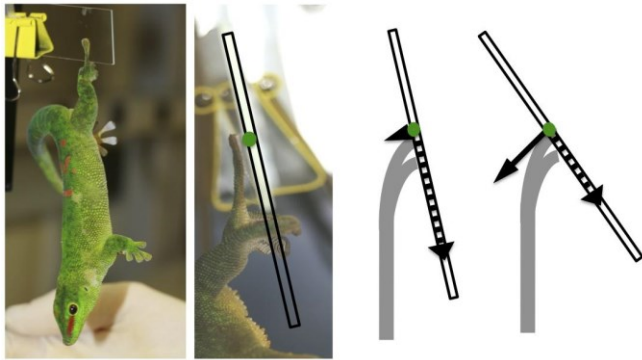
490 Espinoza, JR Wood, Jesse Grismer, Mat Vickers, Andrew Schnell, Scott Harte, Alyssa Stark,
491 Peter Niewiarowski, Ali Dhinojwala, Jonathan Losos, Anthony Herrel, Shane Campbell-Staton,
492 Kristi Fenstermacher, Hannah Frank, Martha Munoz, and Paul VanMiddlesworth for help
493 collecting data in the lab and field, and multiple editors and anonymous reviewers for helpful
494 comments. None of the authors declare any conflicts of interest.

495

496 **Data Accessibility**

497 See Supplemental Material

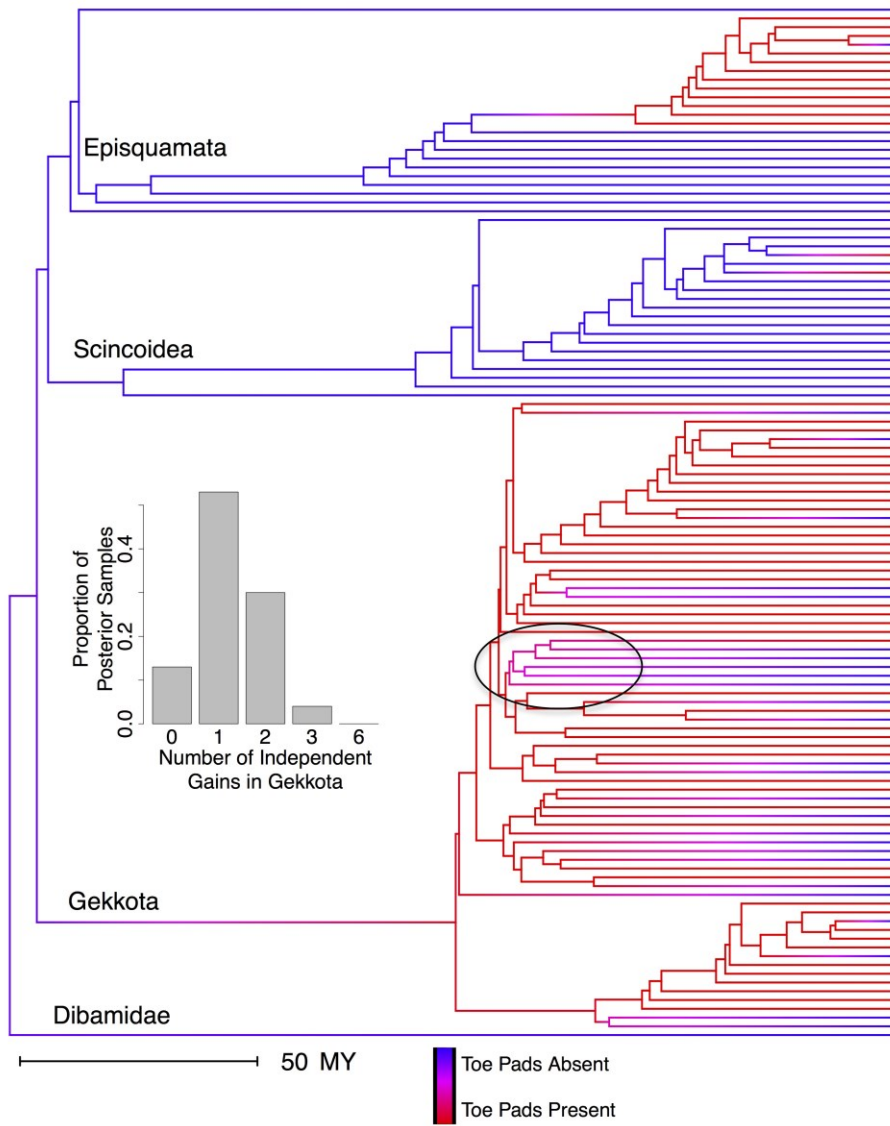
498



500

501 Figure 1. Angle of Toe Detachment Assay. To quantify toe detachment angle, a pad bearing
 502 lizard is suspended from a glass microscope slide by a single rear toe (left images). When the
 503 glass substrate is near vertical, the lizard's toe pad, and hence setae, are predominantly
 504 generating friction relative to the substrate (see right images, seta illustrated in gray, friction
 505 illustrated as dotted arrows). As the substrate is slowly inverted, the setae generate relatively less
 506 friction and more adhesion (see far right image, adhesion illustrated as solid arrow). At the angle
 507 of toe detachment, the setae can no longer maintain the proper orientation with the substrate to
 508 remain attached and the animal falls onto a cushioned base (see video links in Supplemental
 509 Material). As a result, the angle of toe detachment quantifies the maximum amount of adhesion,
 510 relative to friction, generated. Image modified from Hagey et al. (2014).

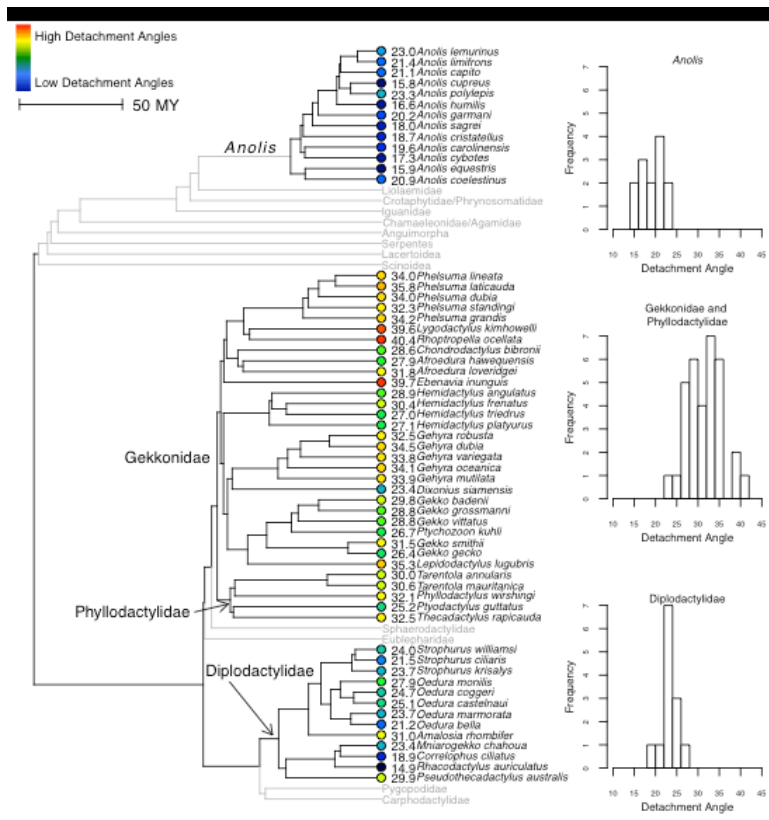
511



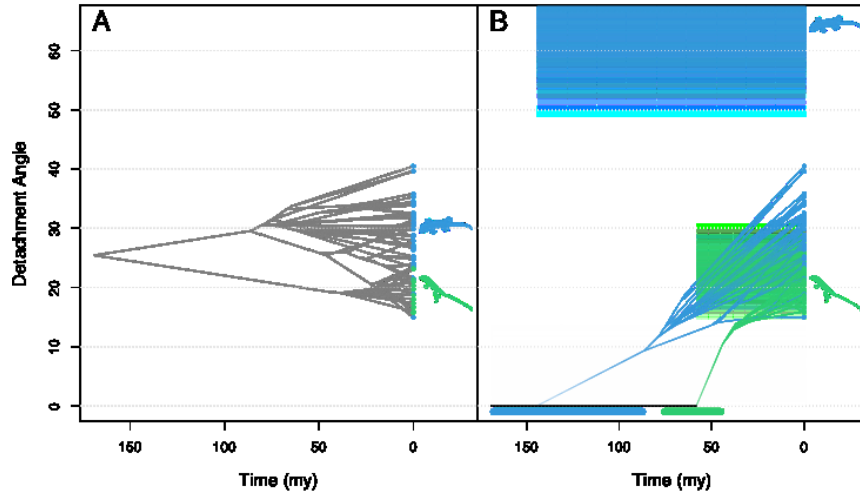
512
513

514 Figure 2. Toe Pad Ancestral State Reconstruction. We reconstructed the presence (red) and
 515 absence (blue) of adhesive toe pads across Squamata. We predicted toe pads likely evolved once
 516 within geckos, with many losses. The embedded histogram highlights the number of independent
 517 origins within Gekkota across our posterior sample of reconstructions (see Methods). Some of
 518 the reconstructions in our posterior sample yielded independent origins of toe pads in the stem
 519 leading to *Hemidactylus* (see Results). The root of the clade containing *Hemidactylus* is circled.
 520 For tip names see Supplemental Material.

521



522
 523 Figure 3. Phylogeny of Focal Padded Species with Performance Data. We quantified toe-
 524 detachment angle across 46 species of geckos and 13 species of anoles. Colored circles and
 525 numbers at the tips of the phylogeny represent each species' estimated detachment angle.
 526 Warmer colors represent higher detachment angles. We display prominent non-padded lizard
 527 groups to emphasize the evolutionary distance between anoles and geckos and to highlight the
 528 fact that not all families of geckos have toe pads (Carphodactylidae and Eublepharidae lack pads,
 529 Pygopodidae lacks limbs). Sphaerodactyls do possess adhesive toe pads, but we did not quantify
 530 their performance. Histograms to the right of the phylogeny illustrate the observed variation in
 531 performance within anoles, diplodactyls, and gekkonids and phyllodactylids. We found *Anolis*
 532 lizards to have the lowest detachment angles, followed by diplodactylids. Gekkonids and
 533 phyllodactylids had the highest and broadest range of detachment angles.
 534

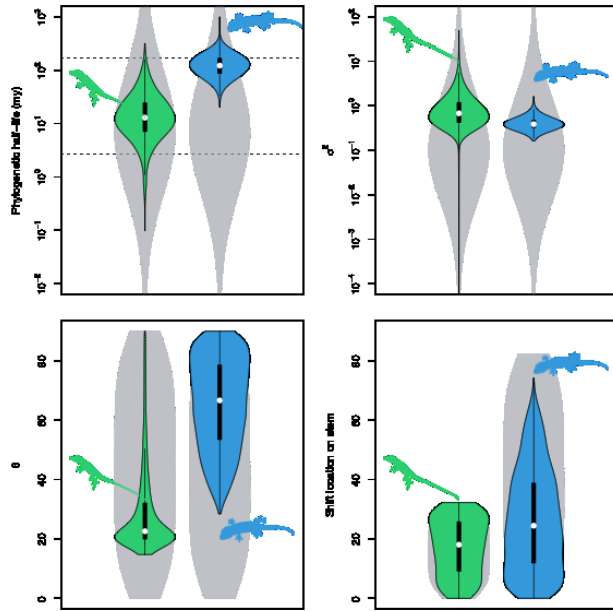


535

536

537 Figure 4. Ancestral state reconstructions using a single-regime BM model (A) and the median
 538 posterior parameter estimates for the $OU\sigma^2\alpha\theta_{\text{Bayesian}}$ model (B) in *bayou*, which assumes
 539 independent origins of toe pads geckos and anoles. Anole data are displayed in green and gecko
 540 data in blue. B) median parameter estimates for the OU target value are indicated by colored
 541 dotted lines within the shaded bands indicating the expected densities of the stationary
 542 distributions. Horizontal bars below the X-axis indicate the constrained shift regions. Note the
 543 median predicted ancestral performance in plot A is estimating a toe detachment angle of
 544 approximately 25° for the shared ancestor of geckos and anoles, which likely lacked toe pads.
 545 See Supplemental Material for additional analyses assuming two origins of toe pads in Gekkota.

546



547

548

549 Figure 5. Posterior distributions from the *OU $\sigma^2\alpha\theta$ Bayesian model. Anole data are displayed in
 550 green on the left of each plot. Gecko data are in blue on the right of each plot. White dots
 551 indicate median estimates for each parameter while black rectangles and whiskers indicate
 552 quartiles of the distribution. Gray violin plots indicate the prior distribution. The upper dotted
 553 line on the phylogenetic half-life plot indicates the root age of the Squamata phylogeny
 554 corresponding roughly to the value at which the OU model approaches a Brownian Motion
 555 model. The lower dotted line represents the value of phylogenetic half-life at which no two
 556 species in either phylogeny would have more than a 0.05% phylogenetic correlation, *i.e.*, the
 557 values at which our model simplifies into a white-noise model with independent, identically
 558 distributed trait values with no effect of phylogeny.

559

560

CO ₂ Model	ABC ₂ Variable	Parameter Values			
		Estim.	s ²	Asympt.	
BM1	0.56	23.5	0.26		
CO ₂ -sp	0.19	2	9.46	23.2	Asympt.
		>99.8	5.26	>1000	Converge
DCM	0.15	2	9.23	191.7	Asympt.
		22.7			Converge
BM2'	0.12	23.5	0.26		Asympt.
		0.26			Converge
EOL	0.12	2	9.26	>1000	
		26.5	0.26		
ODM	0.49	2	9.41	199.8	Asympt.
		45.6		200.4	Converge
CO ₂ -f	0.86	2	9.29	114.0	Asympt.
		22.4	0.29		Converge

NANCO Model	ABC ₂ Variable	Parameter Values					
		Estim.	s ²	Asympt.	μ	Half-Year	
*NANCO ₁ -CO ₂	0.57	25.4	23.7	0.5	-	23.3	Asympt.
		0.0	9.27	-	0.59	23.3	Converge
*NANCO ₂	0.54	0.0	9.27	-	0.54	20.4	Asympt.
						23.3	Converge
*NANCO ₃	0.18	0.0	9.27	-	0.49	23.3	Asympt.
					0.59	23.3	Converge
*NANCO ₄	0.94	25.4	23.1	0.5	-	23.3	Asympt.
		99.0	0.23	200.1		20.6	Converge
*NANCO ₅	0.04	2	9.36	117.0	-	18.3	Asympt.
						49.0	Converge
*NANCO ₆	0.03	2	9.36	117.0	-	18.3	Asympt.
		99.0				49.0	Converge
*NANCO ₇	0.01	2	9.41	1.3	-	21.4	Asympt.
		99.0		10.9		22.3	Converge
*NANCO ₈ -sp	0.01	2	9.39	10.9	-	21.4	Asympt.
		99.0	9.41			22.3	Converge
*NANCO ₉	0.00	2	9.39	-	0.03	9.8	Asympt.
		0.0				9.8	Converge
*NANCO ₁₀ -NANCO ₁₁	-	2	9.46	13.9	-	18.1	Asympt.
		22.6		13.9		18.1	
		(17.1, 41.1)	(9.08, 3.08)	(0.1, 65.4)		(1.8, 32.2)	
		66.7	9.29	23.3		24.5	Converge
		(9.2, 0.60)	(7.1, 247.2)		(0.6, 37.2)		

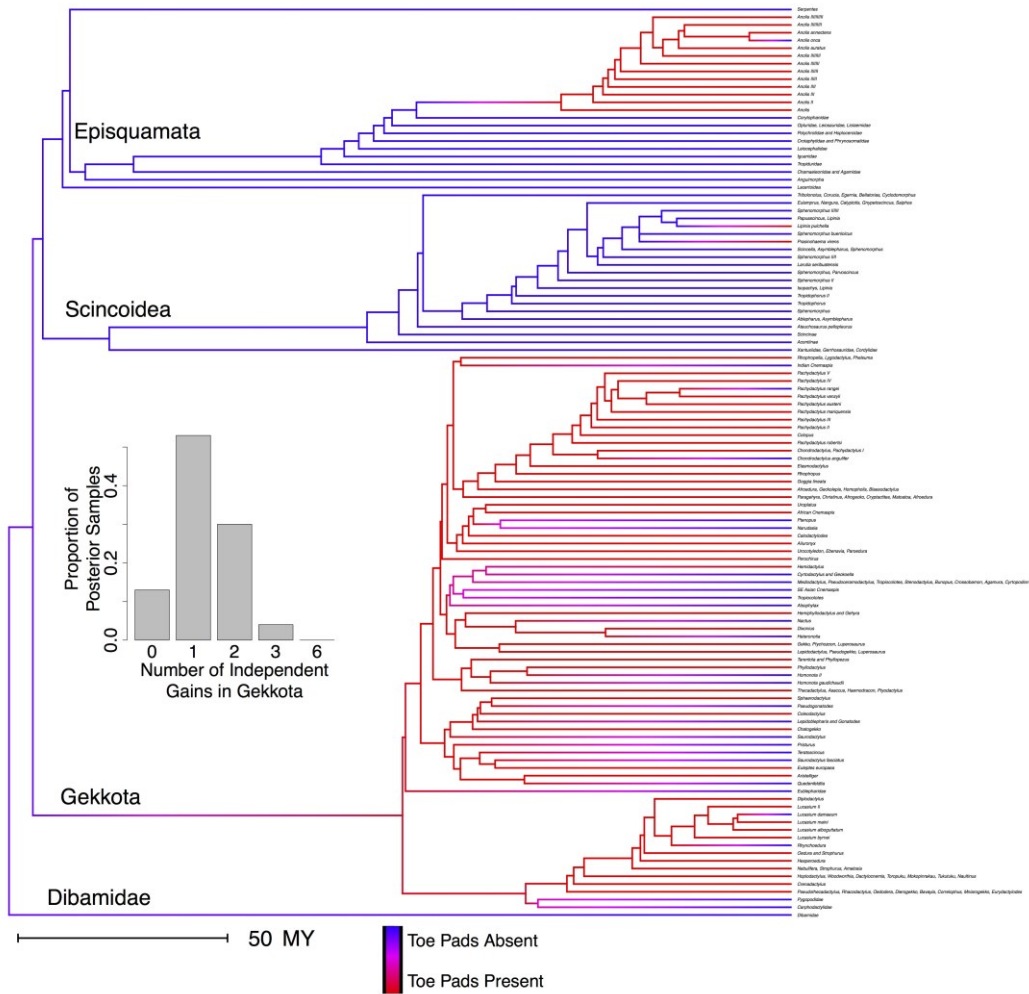
562 Table 1. Model of Trait Evolution Fits and Estimated Parameters. We evaluated multiple models
563 of trait evolution using the OUwie, and *bayou* packages. We ascribed model names based on
564 their use of a BM or OU procedure followed by parameters that were allowed to vary across
565 clades. We display AICc weights and parameter estimates for each model we considered, sorted
566 by their AICc weights. The models considered in our *bayou* analyses all incorporated constraints
567 (denoted by asterisks) limiting the trait value to 0° prior to the stem branches leading to geckos
568 and anoles. We report the predicted timing of the origins of toe pads in geckos and anoles (Shift
569 Time) in millions of years since the split of the stem segregating the clade from the rest of the
570 phylogeny. OU α values are displayed as phylogenetic half-life values ($\ln[2]/\alpha$) in millions of
571 years. Our *bayou* Brownian Motion models also include root parameter values illustrating the
572 trait value at the root of the phylogeny. In BM models lacking a trend, in which the μ parameter
573 is zero, the root parameter value is also the clade mean. The μ parameter represents the expected
574 change in trait over time. Lastly, results from our $*OU\sigma^2\alpha\theta_{\text{Bayesian}}$ model included estimated
575 medians and 95% highest posterior density (HPD) intervals for each parameter, indicated in
576 parentheses under each value, displayed in the last row of the table.
577

578 **Supplemental Material**

579 Here we provide additional information including species level data, links to performance assay
 580 videos, additional results, and a description of how we measured performance in the field using
 581 purpose-built equipment.

582
 583 File S.1. A .xlsx file listing our toe pad presence/absence assignments for all 4162 tips in the
 584 squamate phylogeny from Pyron and Burbrink (2013).

585



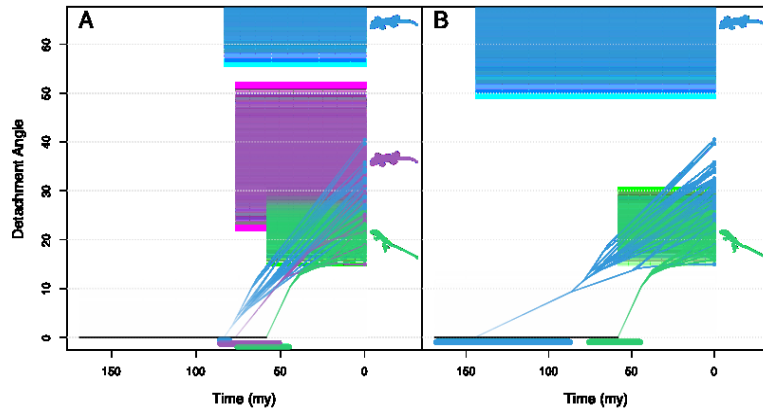
586
 587 Figure S.1 Ancestral State Reconstruction with Tip Names (see Figure 2, Methods, and Results
 588 for additional information)

589

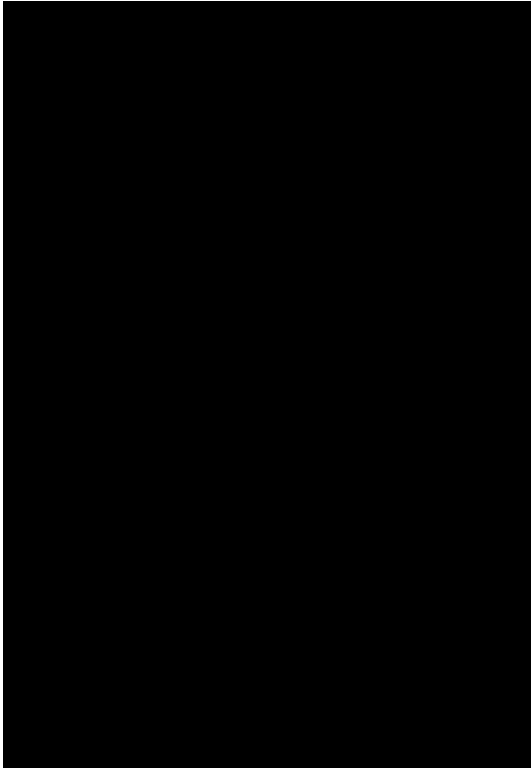
590 *Modeling Trait Evolution Assuming Two Origins of Toe Pads within Gekkota*

591 In addition to analyses assuming a single origin of toe pads within geckos, we considered an
592 additional set of limited analyses assuming two independent origins of toe pads within Gekkota,
593 one origin at the base of the Diplodactylidae family and a second at the base of the
594 Phyllodactylidae and Gekkonidae clade. Our primary goal with these analyses was to determine
595 whether two origins (which received some support in our reconstruction of toe pad evolution)
596 changed our primary conclusions —namely, that Gekkota evolved under BM-like evolution with
597 a trend with limited evidence of constraint.

598 Models fit using Maximum Likelihood to two-origin scenarios recover very similar
599 dynamics, with Brownian motion with a trend being preferred over an OU model (AICs: BM
600 with a trend = 264.3; OU = 296.3). Furthermore, even when an OU model is fit to our two gecko
601 clades, they recover very BM-like dynamics with long phylogenetic half-lives
602 (Gekkonidae/Phyllodactylidae = 136.7 my; Diplodactylidae = 193.0 my). Furthermore, we find
603 little evidence for unique dynamics between the two putative origins (AICs: OU shared
604 parameters = 297.4; OU independent parameters = 296.3), suggesting that the two gecko clades
605 generally evolve under similar dynamics. We visualized our analysis by fitting the OU model
606 described above in a Bayesian framework (left plot) with separate origins for Diplodactylidae
607 (purple) and other Gekkonidae/Phyllodactylidae (blue). Both clades had long half-lives
608 (Gekkonidae/Phyllodactylidae median = 91.5 my; Diplodactylidae median = 64.8 my) and distant
609 optima (Gekkonidae/Phyllodactylidae median [95%CI] = 67.6° [33.3° , 88.8°]; Diplodactylidae
610 geckos median [95%CI] = 46.1° [23.5° , 87.3°]). We compared this model to our Bayesian
611 model from the main text (right plot). Note that although BM with a trend was preferred over OU
612 models, OU models with distant optima and long phylogenetic half-lives approximate BM with a
613 trend. Related to this point, estimates of half-lives are stronger in our Bayesian than the
614 Maximum Likelihood analyses because we constrained the optima values using priors to not
615 exceed 90° in our Bayesian analyses. However, for visualization purposes, we view these
616 differences as minimal. We conclude that even with multiple origins, the data suggest more
617 gradual and unconstrained trait evolution across the geckos than in the *Anolis* lizards.



618
619
620



621
622 Table S.1. Performance Observations. Species mean toe detachment angle and variance
623 (displayed in parentheses). The number of individuals tested was not recorded for some species
624 of anoles (number of individuals = NA) and were treated as observations from a single individual
625 in our analyses.

626
627 File S.2 Performance Observations .xlsx file

628
629 Links illustrating our toe detachment assay on YouTube:
630 Far away view: <https://www.youtube.com/watch?v=4EDUi9If-4c>
631 Close up view: <https://www.youtube.com/watch?v=HC-FdtGqv54>

632

633 *AUTEUR and SURFACE Analyses*

634 In addition to our OUwie and modified *bayou* trait evolution analyses, we also considered BM
635 trait evolution using AUTEUR (Eastman et al. 2011), currently within the *geiger* package, and
636 shifts in the OU target parameter θ (assuming α , the strength of pull towards θ , and the rate of
637 diffusion, σ^2 , are shared across clades) using the R package SURFACE (Ingram and Mahler
638 2013). These analyses each require different *a priori* information and use different model fitting
639 approaches. AUTEUR does not require *a priori* clade assignments and uses a reversible-jump
640 MCMC approach to fit multi-regime BM models, allowing either the rate of change (σ^2), mean
641 trait value (θ), or both parameters to vary between clades. We evaluated models with clade
642 specific σ^2 values ($BM\sigma^2$), clade specific θ values ($BM\theta$), and models in which both θ and σ^2
643 could vary ($BM\sigma^2\theta$), all while including species-level trait value error. For each dataset, we
644 conducted two runs, evaluating chain convergence. All of our AUTEUR runs used one million
645 generations, sampling every five hundred generations.

646 The SURFACE package uses a step-wise AIC approach without *a priori* clade
647 assignments, varying the OU parameter θ for different clades until the AIC score can no longer
648 be improved. This package was designed to identify examples of convergence and so the second
649 phase of the analysis condenses previously identified regimes, allowing parameter values to be
650 shared between clades, and reducing the total number of unique parameter sets. We conducted
651 simulations to determine if the model identified by SURFACE contained a significant number of
652 regimes as compared to the number expected by chance under a single-rate BM model. We
653 simulated 500 datasets under BM using our cropped Pyron and Burbrink (2013) phylogeny. We
654 ran each simulated dataset through the forward and backward phases of SURFACE and tabulated
655 the number of regimes observed to generate a null distribution.

656 The results from our AUTEUR analyses, which considered multi-rate and multi-theta BM
657 models, found no significant changes in rate or mean across clades. All six of our runs, varying
658 σ^2 ($BM\sigma^2$), θ ($BM\theta$), or σ^2 and θ concurrently ($BM\sigma^2\theta$) with two replicates each, estimated
659 similar parameter values ($\sigma^2 = 0.29 \pm 0.005$ SE, $\theta = 25.6 \pm 0.03$ SE, see Table below). We
660 display σ^2 and θ parameter estimates for each of our duplicate simulations (denoted as subscript
661 one or two). We concluded that our duplicate runs were converging by comparing σ^2 and θ
662 posterior probabilities of each branch between duplicated runs, finding them to be similar. We
663 also used the Heidelberger and Welch convergence diagnostic, which includes the Cramer-von-

664 Mises statistic and the half-width test. In all of our analyses, the root and log-likelihood
 665 parameters passed both tests. We found effective sizes ranging from 598 to 2104 for our root and
 666 log-likelihood parameters across all our runs, which take into account autocorrelation between
 667 successive MCMC chain samples.

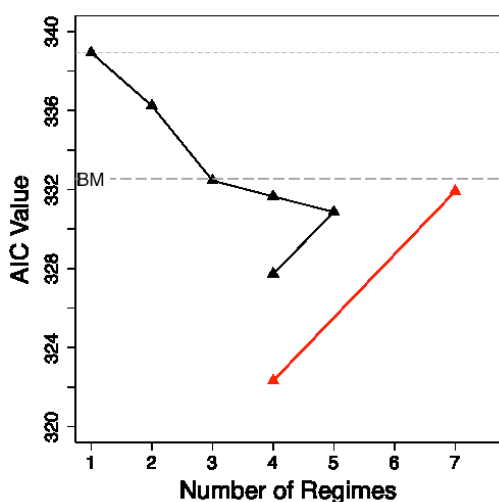
AICTEUR		
Model	σ^2	θ
BM σ_1	0.31	25.5
BM σ_2	0.31	25.5
BM σ_1^2	0.29	25.6
BM σ_2^2	0.29	25.7
BM $\sigma_1^2\theta_1$	0.28	25.6
BM $\sigma_2^2\theta_2$	0.29	25.6

668
 669

670 Our SURFACE analyses originally found a multi- θ OU model with five regimes
 671 condensed into four made up of anoles and diplodactylid geckos, gekkonids and phyllodactylids,
 672 *Rhacodactylus auriculatus*, and three gekkonid species, *Lygodactylus kimhowelli*, *Rhoptropella*
 673 *ocellata*, and *Ebenavia inunguis*. Below we display parameter estimates and AIC scores for
 674 single-regime BM and OU (BM1 and OU1), and uncondensed and condensed models. During
 675 the stepwise SURFACE analysis our model AIC scores dropped as more regimes were added
 676 (black triangles; see Figure and Table below), starting at a single-theta OU model (upper dotted
 677 line, AIC = 338.9), until the analysis settled on a five-regime model (AIC = 330.9), scoring
 678 lightly better than a single-regime BM model (lower dashed line, AIC = 332.5). The analyses
 679 then looked for improvements to the AIC score by condensing regimes. By condensing the two
 680 small regimes within Gekkonidae into one, the AIC score and number of unique regimes were
 681 reduced to four and an AIC of 327.7. Although, when we consider the number of regimes
 682 expected under a single-rate BM model, we see that five regimes with one condensation event
 683 could easily occur by chance. In our 500 simulated datasets under single-rate BM, we found an
 684 average of 5.3 regimes, a mode of five, and a maximum of 11 regimes, with an average of 2.0
 685 convergence events, a mode of two, and a maximum of six convergence events. These
 686 simulations suggest that a multi-theta OU model like the one we observed fitting our data best
 687 may have a low AIC score (327.7), but it is a pattern that can easily appear under a single-rate
 688 BM model (AIC = 332.5).

689 Considering the fact that our SURFACE analyses successfully fit divergent species to
 690 their own regimes (*Rhacodactylus auriculatus*, *Lygodactylus kimhowelli*, *Rhoptropella ocellata*,

691 and *Ebenavia inunguis*), we conducted a further analysis, manually condensing high performing
 692 diplodacylid geckos (*Amalosia rhombifer* and *Pseudotoecadactylus australis*) into the gekkonid
 693 regime and recalculated the AIC score for this new, further condensed, model (red triangles; see
 694 Figure and Table below). We found our uncondensed seven-regime model had a higher AIC
 695 (331.9) as compared to the non-condensed five-regime model SURFACE found, yet when we
 696 condensed our modified model into four regimes, its AIC score (322.3) dropped well below the
 697 best condensed four-regime model identified by SURFACE. We believe this model was not
 698 chosen by the initial SURFACE analysis due the stepwise AIC approach SURFACE uses.
 699



SURFACE Model	AIC	σ^2	n	g
BM1	332.54	0.29	NA	25.4
OU1	338.93	0.33	0.003	25.7
OU3 _{Condensed}	330.86	0.33	0.013	22.1 - Anolis, Diplodactylidae 33.2 - Gekkonidae, Phyllodactylidae 49.3 - Lygodactylus, Rhoptropella -8.2 - Rhacodactylus 48.1 - Ebenaria
OU3 _{Condensed}	327.73	0.33	0.013	22.1 - Anolis, Diplodactylidae 33.2 - Gekkonidae, Phyllodactylidae 48.8 - Lygodactylus, Rhoptropella, Ebenaria -8.2 - Rhacodactylus
OU3 _{Manual Condensed}	331.91	0.31	0.016	20.8 - Anolis, Diplodactylidae 33.0 - Gekkonidae, Phyllodactylidae 47.0 - Lygodactylus, Rhoptropella -0.3 - Rhacodactylus 46.0 - Ebenaria 39.7 - Amalosia 36.0 - Pseudotoecadactylus
OU3 _{Manual Condensed}	322.32	0.34	0.018	20.7 - Anolis, Diplodactylidae 32.8 - Gekkonidae, Phyllodactylidae, Amalosia, Pseudotoecadactylus 45.5 - Lygodactylus, Rhoptropella, Ebenaria 1.2 - Rhacodactylus

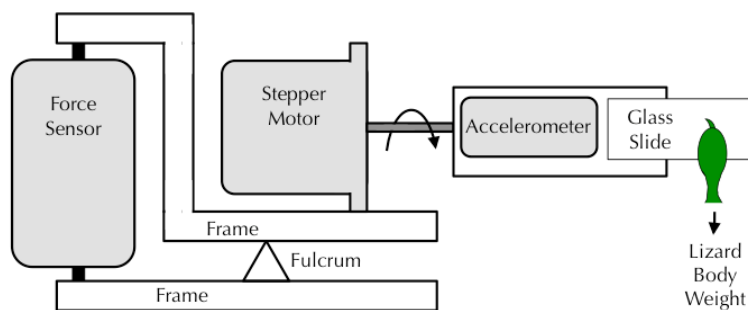
700
 701
 702

703 *Measuring Performance in the Field*

704 Pad bearing lizards with higher detachment angles can likely use highly angled or inverted
705 perches more easily, whereas species with lower detachment angles likely struggle to generate as
706 much adhesion relative to friction and thus may be limited to vertical perches, although toe
707 orientation and foot shape likely play a large role in inverted locomotion. In addition, there may
708 exist a trade-off in high and low detachment angles regarding the production of friction versus
709 adhesion. Species with a high detachment angle likely have setae and spatulae shaped to
710 maintain proper contact with a substrate under high setal shaft angles, producing some amount of
711 both adhesion and friction, but less absolute friction than if the setal shaft angle was near parallel
712 with the substrate, translating the applied force into only friction (also see Pesika et al. 2007).
713 Additional research considering the setal mechanics underlying detachment angle would be
714 necessary to further describe this potential trade-off. In addition, rough surfaces offer a reduced
715 surface area for a padded lizard to attach to, and as a result, higher detachment angles may allow
716 setae to properly attach to the valleys and peaks of a rough surface (Sitti and Fearing 2003;
717 Gillies and Fearing 2014; Gillies et al. 2014).

718 As part of this study, gecko performance was collected in Queensland, Australia using
719 purpose-built equipment consisting of a Pacific Scientific Powermax 1.8° stepper motor (model
720 #P21NRXB-LNN-NS-00), Vernier dual-range force sensor, Vernier three-axis accelerometer,
721 Vernier sensorDAQ data-acquisition interface, and a Phidget bipolar stepper control board
722 (#1063_1). Operation and data collection used a custom LabVIEW program (2011 version
723 11.0.1f2, National Instruments, Austin, TX, USA) running on a Gateway LT series netbook
724 (LT2805u). The frame of our toe detachment equipment was custom-built and acted as a lever
725 with a fulcrum in the center, force sensor at one end, and the lizard suspended from the other end
726 (Fig. S.2).

727



728

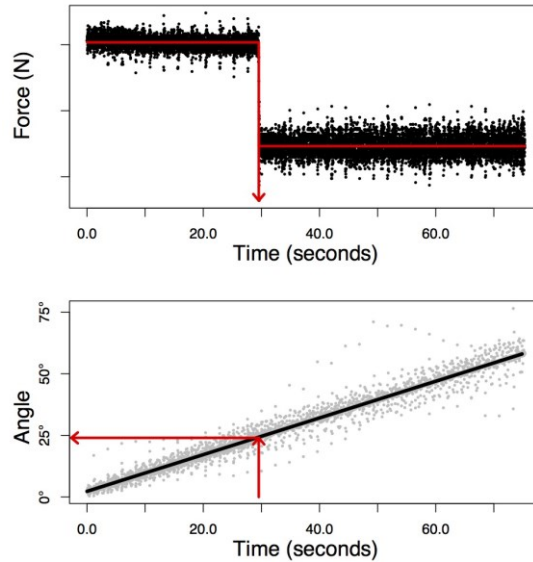
729 Figure S.2. Toe Detachment Field Equipment. We build a field-capable TAD device consisting
730 of a force sensor, stepper motor, and multi-axis accelerometer. The upper frame of our apparatus
731 acts as a lever with the fulcrum, allowing the force sensor (left side of image) to detect when a
732 lizard detaches from the glass (right side of image). Our glass slide and accelerometer were
733 attached to a large flat plate. The accelerometer was positioned to measure acceleration in the Y
734 direction (vertical in our image) and Z direction (perpendicular to the mounting surface, out of
735 the plane of the image, towards the reader).

736

737 An accelerometer, attached to the rotating glass surface, allowed us to determine the angle of the
738 glass surface throughout the course of each trial. Raw toe detachment data consisted of three
739 variables recorded over the course of each trial (acceleration in Y and Z directions and force). By
740 calculating the arctangent of the ratio of the two acceleration measurements perpendicular to the
741 axis of rotation, we could determine angle (Fig. S.2). When rotating, acceleration due to gravity
742 was not linear; rather it changed slowly when near vertical. When near horizontal, acceleration
743 due to gravity changed quickly.

744 Our force sensor recorded the corresponding change in force (Fig. S.3) and allowed us to
745 pinpoint the instant the lizard detaches during a trial. We fit a three-parameter broken regression
746 model to our force output data to pinpoint the moment the lizard detached (Fig. S.3). We
747 estimated the y-intercept of a horizontal line fit to the force data before the lizard fell, the time
748 point at which the lizard fell, and the y-intercept of a horizontal line fit to the force data after the
749 lizard detached (Fig. S.3). Using our estimated time of detachment and our angle data (calculated
750 from accelerometer data), we estimated the angle of the glass at the time of detachment (Fig.
751 S.3).

752



753
 754 Figure S.3. Representative Toe Detachment Performance Trial. Representative data output from
 755 a single toe detachment trial is displayed. Time is on the X-axis. Raw force data (upper plot)
 756 displays our two estimated y-intercepts (red horizontal lines) and time of detachment (red
 757 vertical line, approximately 30 seconds in this example) estimated by a broken regression
 758 analysis. Raw acceleration data were used to estimate the angle of the glass slide through time
 759 (lower plot, gray points). The black line in our lower plot is the estimated substrate angle over
 760 the course of the trial. Our estimated angle of toe detachment is the point in which our estimated
 761 time of detachment intersects with our estimated angle, slightly under 25° in this example.
 762

763 **Work Cited**

- 764 Arnold, S. J. 1983. Morphology, performance and fitness. *Am Zool* 23:347-361.
- 765 Austin, C. C. 1998. Phylogenetic relationships of *Lipinia* (Scincidae) from New Guinea based on
766 DNA sequence variation from the mitochondrial 12S rRNA and nuclear c-mos genes.
767 *HAMADRYAD-MADRAS-* 23:93-102.
- 768 Autumn, K., A. Dittmore, D. Santos, M. Spenko, and M. Cutkosky. 2006a. Frictional adhesion: a
769 new angle on gecko attachment. *J. Exp. Biol.* 209:3569-3579.
- 770 Autumn, K., S. T. Hsieh, D. M. Dudek, J. Chen, C. Chitaphan, and R. J. Full. 2006b. Dynamics
771 of geckos running vertically. *J. Exp. Biol.* 209:260-272.
- 772 Autumn, K., P. H. Niewiarowski, and J. B. Puthoff. 2014. Gecko adhesion as a model system for
773 integrative biology, interdisciplinary science, and bioinspired engineering. *Annu Rev*
774 *Ecol Evol S* 45:445-470.
- 775 Bauer, A. M. 1998. Morphology of the adhesive tail tips of carphodactyline geckos (Reptilia:
776 Diplodactylidae). *J Morphol* 235:41-58.
- 777 Bauer, A. M. and A. P. Russell. 1988. Morphology of gekkonid cutaneous sensilla, with
778 comments on function and phylogeny in the Carphodactylini (Reptilia: Gekkonidae).
779 *Can. J. Zool* 66:1583-1588.
- 780 Beaulieu, J. M., D. C. Jhwueng, C. Boettiger, and B. C. O'Meara. 2012. Modeling Stabilizing
781 Selection: Expanding the Ornstein-Uhlenbeck Model of Adaptive Evolution. *Evolution*
782 66:2369-2383.
- 783 Beaulieu, J. M. and B. C. O'Meara. 2016. Detecting Hidden Diversification Shifts in Models of
784 Trait-Dependent Speciation and Extinction. *Syst Biol* 65:583-601.
- 785 Beaulieu, J. M., B. C. O'Meara, and M. J. Donoghue. 2013. Identifying hidden rate changes in
786 the evolution of a binary morphological character: the evolution of plant habit in
787 campanulid angiosperms. *Syst Biol* 62:725-737.
- 788 Brown, D., J. W. Wilmer, and S. Macdonald. 2012. A revision of *Strophurus taenicauda*
789 (Squamata; Diplodactylidae) with the description of two new subspecies from central
790 Queensland and a southerly range extension. *Zootaxa*:1-28.
- 791 Burnham, K. P. and D. R. Anderson. 2002. Model selection and multi-model inference: a
792 practical information-theoretic approach. Springer, New York, NY.

793 Butler, M. A. and A. A. King. 2004. Phylogenetic comparative analysis: A modeling approach
794 for adaptive evolution. *Am. Nat.* 164:683-695.

795 Crandell, K. E., A. Herrel, M. Sasa, J. B. Losos, and K. Autumn. 2014. Stick or grip? Co-
796 evolution of adhesive toepads and claws in *Anolis* lizards. *Zoology* 117:363-369.

797 Davis, M. P., P. E. Midford, and W. Maddison. 2013. Exploring power and parameter estimation
798 of the BiSSE method for analyzing species diversification. *Bmc Evol Biol* 13.

799 Daza, J. D., A. M. Bauer, and E. D. Snively. 2014. On the fossil record of the Gekkota. *Anat Rec*
800 (Hoboken) 297:433-462.

801 Daza, J. D., E. L. Stanley, P. Wagner, A. M. Bauer, and D. A. Grimaldi. 2016. Mid-Cretaceous
802 amber fossils illuminate the past diversity of tropical lizards. *Sci Adv* 2:e1501080.

803 Eastman, J. M., M. E. Alfaro, P. Joyce, A. L. Hipp, and L. J. Harmon. 2011. A novel
804 comparative method for identifying shifts in the rate of character evolution on trees.
805 *Evolution* 65:3578-3589.

806 Eastman, J. M., D. Wegmann, C. Leuenberger, and L. J. Harmon. 2013. Simpsonian 'Evolution
807 by Jumps' in an adaptive radiation of *Anolis* lizards. arXiv preprint arXiv:1305.4216.

808 Emerson, S. B. 1991. The Ecomorphology of Bornean Tree Frogs (Family Rhacophoridae). *Zool*
809 *J Linn Soc-Lond* 101:337-357.

810 FitzJohn, R. G. 2012. Diversitree: comparative phylogenetic analyses of diversification in R.
811 *Methods Ecol Evol* 3:1084-1092.

812 Gamble, T., E. Greenbaum, T. R. Jackman, A. P. Russell, and A. M. Bauer. 2012. Repeated
813 origin and loss of adhesive toepads in geckos. *PLoS ONE* 7:e39429.

814 Gamble, T., E. Greenbaum, T. R. Jackman, A. P. Russell, and A. M. Bauer. 2017. Repeated
815 evolution of digital adhesion in geckos, a reply to Harrington and Reeder. *J Evol Biol.*

816 Garcia-Porta, J. and T. J. Ord. 2013. Key innovations and island colonization as engines of
817 evolutionary diversification: a comparative test with the Australasian diplodactyloid
818 geckos. *J Evol Biol* 26:2662-2680.

819 Haacke, W. 1976. The burrowing geckos of southern Africa, 5 (Reptilia: Gekkonidae). *Annals of*
820 *the Transvaal Museum* 30:71-89.

821 Hagey, T. J., J. B. Puthoff, K. E. Crandell, K. Autumn, and L. J. Harmon. 2016. Modeling
822 observed animal performance using the Weibull distribution. *J Exp Biol* 219:1603-1607.

823 Hagey, T. J., J. B. Puthoff, M. Holbrook, L. J. Harmon, and K. Autumn. 2014. Variation in setal
824 micromechanics and performance of two gecko species. *Zoomorphology* 133:111-126.

825 Hansen, T. F. 1997. Stabilizing selection and the comparative analysis of adaptation. *Evolution*
826 51:1341-1351.

827 Hansen, W. R. and K. Autumn. 2005. Evidence for self-cleaning in gecko setae. *Proc. Natl.*
828 *Acad. Sci. USA* 102:385-389.

829 Harmon, L. J., J. Baumes, C. Hughes, J. Soberon, C. D. Specht, W. Turner, C. Lisle, and R. W.
830 Thacker. 2013. *Arbor: Comparative Analysis Workflows for the Tree of Life*. PLoS
831 *Currents* 5:ecurrents.tol.099161de099165eabdee099073fd099163d099121a044518dc.

832 Harmon, L. J., J. A. Schulte, A. Larson, and J. B. Losos. 2003. Tempo and mode of evolutionary
833 radiation in iguanian lizards. *Science* 301:961-964.

834 Harmon, L. J., J. T. Weir, C. D. Brock, R. E. Glor, and W. Challenger. 2008. GEIGER:
835 investigating evolutionary radiations. *Bioinformatics* 24:129-131.

836 Harrington, S. and T. W. Reeder. 2017. Rate heterogeneity across Squamata, misleading
837 ancestral state reconstruction and the importance of proper null model specification. *J*
838 *Evol Biol* 30:313-325.

839 Higham, T. E., A. V. Birn-Jeffery, C. E. Collins, C. D. Hulsey, and A. P. Russell. 2015. Adaptive
840 simplification and the evolution of gecko locomotion: Morphological and biomechanical
841 consequences of losing adhesion. *Proc Natl Acad Sci U S A* 112:809-814.

842 Higham, T. E., T. Gamble, and A. P. Russell. 2016. On the origin of frictional adhesion in
843 geckos: small morphological changes lead to a major biomechanical transition in the
844 genus *Gonatodes*. *Biol J Linn Soc*.

845 Hu, S. H., S. Lopez, P. H. Niewiarowski, and Z. H. Xia. 2012. Dynamic self-cleaning in gecko
846 setae via digital hyperextension. *J R Soc Interface* 9:2781-2790.

847 Huber, G., S. N. Gorb, N. Hosoda, R. Spolenak, and E. Arzt. 2007. Influence of surface
848 roughness on gecko adhesion. *Acta Biomater.* 3:607-610.

849 Ingram, T. and D. L. Mahler. 2013. SURFACE: detecting convergent evolution from
850 comparative data by fitting Ornstein-Uhlenbeck models with stepwise Akaike
851 Information Criterion. *Methods Ecol Evol* 4:416-425.

852 Irish, F. J., E. E. Williams, and E. Seling. 1988. Scanning electron microscopy of changes in
853 epidermal structure occurring during the shedding cycle in squamate reptiles. *J Morphol*
854 197:105-126.

855 Irschick, D. J., C. C. Austin, K. Petren, R. N. Fisher, J. B. Losos, and O. Ellers. 1996. A
856 comparative analysis of clinging ability among pad-bearing lizards. *Biol. J. Linn. Soc.*
857 59:21-35.

858 Irschick, D. J., A. Herrel, and B. Vanhooydonck. 2006. Whole-organism studies of adhesion in
859 pad-bearing lizards: creative evolutionary solutions to functional problems. *J. Comp.*
860 *Physiol. A* 192:1169-1177.

861 Irschick, D. J., L. J. Vitt, P. A. Zani, and J. B. Losos. 1997. A comparison of evolutionary
862 radiations in mainland and Caribbean *Anolis* lizards. *Ecology* 78:2191-2203.

863 Johnson, M. K. and A. P. Russell. 2009. Configuration of the setal fields of *Rhoptropus*
864 (*Gekkota*: *Gekkonidae*): functional, evolutionary, ecological and phylogenetic
865 implications of observed pattern. *J Anat* 214:937-955.

866 Lande, R. 1976. Natural-selection and random genetic drift in phenotypic evolution. *Evolution*
867 30:314-334.

868 Losos, J. B. 2009. *Lizards in an evolutionary tree : the ecology of adaptive radiation in anoles.*
869 University of California Press, Berkeley.

870 Macrini, T. E., D. J. Irschick, and J. B. Losos. 2003. Ecomorphological differences in toepad
871 characteristics between mainland and island anoles. *J Herpetol* 37:52-58.

872 Maddison, W. P. 2006. Confounding asymmetries in evolutionary diversification and character
873 change. *Evolution* 60:1743-1746.

874 Maddison, W. P. and R. G. FitzJohn. 2015. The unsolved challenge to phylogenetic correlation
875 tests for categorical characters. *Syst Biol* 64:127-136.

876 Maddison, W. P., P. E. Midford, and S. P. Otto. 2007. Estimating a binary character's effect on
877 speciation and extinction. *Syst Biol* 56:701-710.

878 Maderson, P. 1970. Lizard hands and lizard glands: models for evolutionary study. *Forma et*
879 *Functio* 3:179-204.

880 Maderson, P. F. A. 1964. Keratinized epidermal derivatives as an aid to climbing in gekkonid
881 lizards. *Nature* 203:780-781.

882 McCool, J. I. 2012. Using the Weibull distribution: Reliability, modeling and inference. Wiley,
883 Hoboken, NJ.

884 Mitchell, J. S. 2015. Extant-only comparative methods fail to recover the disparity preserved in
885 the bird fossil record. *Evolution* 69:2414-2424.

886 Moen, D. S., D. J. Irschick, and J. J. Wiens. 2013. Evolutionary conservatism and convergence
887 both lead to striking similarity in ecology, morphology and performance across
888 continents in frogs. *P R Soc B* 280.

889 Nicholson, K. E., A. Mijares-Urrutia, and A. Larson. 2006. Molecular phylogenetics of the
890 *Anolis onca* series: a case history in retrograde evolution revisited. *J Exp Zool B Mol Dev*
891 *Evol* 306:450-459.

892 Oliver, P. M., A. M. Bauer, E. Greenbaum, T. Jackman, and T. Hobbie. 2012. Molecular
893 phylogenetics of the arboreal Australian gecko genus *Oedura* Gray 1842 (Gekkota:
894 Diplodactylidae): another plesiomorphic grade? *Mol Phylogenet Evol* 63:255-264.

895 Oliver, P. M. and P. Doughty. 2016. Systematic revision of the marbled velvet geckos (*Oedura*
896 *marmorata* species complex, Diplodactylidae) from the Australian arid and semi-arid
897 zones. *Zootaxa* 4088:151-176.

898 Peattie, A. M. 2007. The Function and Evolution of Gekkotan Adhesive Feet. Pp. 61. University
899 of California, Berkeley, PhD Dissertation.

900 Peattie, A. M. 2008. Subdigital setae of narrow-toed geckos, including a eublepharid
901 (*Aeluroscalabotes felinus*). *Anat Rec* 291:869-875.

902 Pennell, M. W., J. M. Eastman, G. J. Slater, J. W. Brown, J. C. Uyeda, R. G. FitzJohn, M. E.
903 Alfaro, and L. J. Harmon. 2014. geiger v2.0: an expanded suite of methods for fitting
904 macroevolutionary models to phylogenetic trees. *Bioinformatics* 30:2216-2218.

905 Persson, B. N. J. 2007. Biological adhesion for locomotion: basic principles. *J. Adhesion Sci.*
906 *Technol.* 21:1145-1173.

907 Peterson, J. A. 1983. The evolution of the subdigital pad in *Anolis*. I. Comparisons among the
908 anoline genera. *Advances in herpetology and evolutionary biology: essays in honor of*
909 *Ernest E. Williams*:245-283.

910 Peterson, J. A. 1984. The microstructure of the scale surface in iguanid lizards. *J Herpetol*:437-
911 467.

912 Peterson, J. A. and E. E. Williams. 1981. A case history in retrograde evolution: the *Onca*
913 lineage in anoline lizards. II. Subdigital fine structure. Bull. Mus. Comp. Zool. 149:215-
914 268.

915 Pianka, E. R. and S. L. Sweet. 2005. Integrative biology of sticky feet in geckos. BioEssays
916 27:647-652.

917 Pugno, N. M. and E. Lepore. 2008a. Living Tokay geckos display adhesion times following
918 Weibull Statistics. J. Adhesion 84:949-962.

919 Pugno, N. M. and E. Lepore. 2008b. Observation of optimal gecko's adhesion on nanorough
920 surfaces. BioSystems 94:218-222.

921 Pyron, R. A. and F. T. Burbrink. 2013. Early origin of viviparity and multiple reversions to
922 oviparity in squamate reptiles. Ecol Lett 17:13-21.

923 Rabosky, D. L. and E. E. Goldberg. 2015. Model inadequacy and mistaken inferences of trait-
924 dependent speciation. Syst Biol 64:340-355.

925 Rabosky, D. L. and E. E. Goldberg. 2017. FiSSE: A simple nonparametric test for the effects of a
926 binary character on lineage diversification rates. Evolution.

927 Revell, L. J. 2012. phytools: an R package for phylogenetic comparative biology (and other
928 things). Methods Ecol Evol 3:217-223.

929 Ruibal, R. 1968. The ultrastructure of the surface of lizard scales. Copeia 1968:698-703.

930 Ruibal, R. and V. Ernst. 1965. The structure of the digital setae of lizards. J. Morphol. 117:271-
931 293.

932 Russell, A. P. 1976. Some comments concerning interrelationships among gekkonine geckos. Pp.
933 217-244 in A. d. A. B. a. C. B. Cox, ed. Morphology and Biology of the Reptiles.
934 Linnean Society Symposium Series Number 3. Academic Press, London.

935 Russell, A. P. 1979. Parallelism and integrated design in the foot structure of gekkonine and
936 diplodactyline geckos. Copeia 1979:1-21.

937 Russell, A. P. 2002. Integrative Functional Morphology of the Gekkotan Adhesive System
938 (Reptilia: Gekkota). Integr. Comp. Biol. 42:1154-1163.

939 Russell, A. P., J. Baskerville, T. Gamble, and T. E. Higham. 2015. The evolution of digit form in
940 *Gonatodes* (Gekkota: Sphaerodactylidae) and its bearing on the transition from frictional
941 to adhesive contact in gekkotans. J Morphol 276:1311-1332.

942 Russell, A. P. and A. M. Bauer. 1988. Paraphalangeal elements of gekkonid lizards: a
943 comparative survey. *J Morphol* 197:221-240.

944 Russell, A. P. and M. K. Johnson. 2007. Real-world challenges to, and capabilities of, the
945 gekkotan adhesive system: contrasting the rough and the smooth. *Can. J. Zool.* 85:1228-
946 1238.

947 Russell, A. P. and M. K. Johnson. 2014. Between a rock and a soft place: microtopography of the
948 locomotor substrate and the morphology of the setal fields of Namibian day geckos
949 (Gekkota: Gekkonidae: *Rhoptropus*). *Acta Zool* 95:299-318.

950 Sadlier, R. A., D. O'Meally, and G. M. Shea. 2005. A new species of spiny-tailed gecko
951 (Squamata: Diplodactylidae: *Strophurus*) from Inland Queensland. *Mem. Queensl. Mus.*
952 51:573-582.

953 Sherratt, E., M. del Rosario Castañeda, R. J. Garwood, D. L. Mahler, T. J. Sanger, A. Herrel, K.
954 de Queiroz, and J. B. Losos. 2015. Amber fossils demonstrate deep-time stability of
955 Caribbean lizard communities. *Proc. Natl. Acad. Sci.* 112:9961-9966.

956 Stark, A. Y., T. W. Sullivan, and P. H. Niewiarowski. 2012. The effect of surface water and
957 wetting on gecko adhesion. *J Exp Biol* 215:3080-3086.

958 Stewart, G. R. and R. S. Daniel. 1972. Scales of Lizard Gekko-Gecko - Surface-Structure
959 Examined with Scanning Electron-Microscope. *Copeia*:252-&.

960 Stewart, G. R. and R. S. Daniel. 1975. Microornamentation of lizard scales: some variations and
961 taxonomic correlations. *Herpetologica* 31:117-130.

962 Tian, Y., N. Pesika, H. Zeng, K. Rosenberg, B. Zhao, P. McGuiggan, K. Autmn, and J.
963 Israelachvili. 2006. Adhesion and friction in gecko toe attachment and detachment. *Proc.*
964 *Natl. Acad. Sci. USA* 103:19320-19325.

965 Title, P. O. and D. L. Rabosky. 2016. Do Macrophylogenies Yield Stable Macroevolutionary
966 Inferences? An Example from Squamate Reptiles. *Syst Biol.*

967 Underwood, G. 1954. On the classification and evolution of geckos. *Proc Zool Soc Lond*
968 124:469-492.

969 Uyeda, J. C. and L. J. Harmon. 2014. A novel Bayesian method for inferring and interpreting the
970 dynamics of adaptive landscapes from phylogenetic comparative data. *Syst Biol* 63:902-
971 918.

972 Vanhooydonck, B., A. Andronescu, A. Herrel, and D. J. Irschick. 2005. Effects of substrate
973 structure on speed and acceleration capacity in climbing geckos. *Biol J Linn Soc* 85:385-
974 393.

975 Vucko, M. J. 2008. The dynamics of water on the skin of Australian carphodactyline and
976 diplodactyline geckos. Pp. 166. School of Marine and Tropical Biology. James Cook
977 University, Townsville, Queensland, Australia, Masters Thesis.

978 Wainwright, P. C. and S. M. Reilly. 1994. *Ecological Morphology*. University of Chicago Press,
979 Chicago IL.

980 Williams, E. E. and J. A. Peterson. 1982. Convergent and alternative designs in the digital
981 adhesive pads of scincid lizards. *Science* 215:1509-1511.

982 Wilson, S. and G. Swan. 2010. *Complete Guide to Reptiles of Australia*, 3rd ed. New Holland
983 Publishers, Chatswood, N.S.W.

984 Yoder, J. B., E. Clancey, S. Des Roches, J. M. Eastman, L. Gentry, W. Godsoe, T. J. Hagey, D.
985 Jochimsen, B. P. Oswald, J. Robertson, B. A. J. Sarver, J. J. Schenk, S. F. Spear, and L. J.
986 Harmon. 2010. Ecological opportunity and the origin of adaptive radiations. *J Evol Biol*
987 23:1581-1596.

988 Zenil-Ferguson, R. and M. W. Pennell. 2017. Digest: Trait-dependent diversification and its
989 alternatives. *Evolution*.

990